International Journal of Modern Physics B
Vol. 27, No. 13 (2013) 1350053 (17 pages)

DOI: 10.1142/S0217979213500537

World Scientific
www.worldscientific.com

# ELECTRONIC AND OPTICAL PROPERTIES OF NITROGEN DOPED SiC NANOCRYSTALS: FIRST PRINCIPLES STUDY

MASOUD BEZI JAVAN

*Department of Physics, Faculty of Sciences,*
*Golestan University, Gorgan, Iran*
*javan.masood@gmail.com*

Received 4 December 2012
Revised 17 January 2013
Accepted 30 January 2013
Published 30 April 2013



A typical nitrogen doped spherical SiC nanocrystal with a diameter of 1.2 nm ($Si_{43}C_{44}H_{76}$) using linear combination atomic orbital (LCAO) in combination with pseudopotential density functional calculation have been studied. Our selected SiC nanocrystal has been modeled taking all the cubic bulk SiC atoms contained within a sphere of a given radius and terminating the surface dangling bonds with hydrogen atoms. We have examined nine possible situations in which nitrogen has a high probability for replacement in the lattice or placed between atoms in the nanocrystal. We have found that the silicone can substitute with a nitrogen atom in each layer as the constructed nanocrystals remain thermodynamically stable. Also the nitrogen atom can be placed between the free atomic spaces as the more thermodynamically stable position of the nitrogen is between the topmost layers. Also the optical absorption and refractive index energy dispersions of the pure and various stable doped SiC nanocrystals were studied.

*Keywords*: Nanocrystal; silicone carbide; optical absorption; refractive index.

PACS numbers: 31.15.A-, 78.20.Ci, 78.66.Jg

## 1. Introduction

Entering the range of the nanotechnology has provided many researches and applications for semiconductor nanostructures. Large band-gap materials offer interesting properties required for optoelectronic devices. Such devices are especially attractive for ultraviolet radiation detection, as semiconductor materials with band gaps larger than that of silicone can be produced and used as "solar-blind" detectors that are not affected by daylight. Silicone carbide (SiC) as one of the most important wide band gap semiconductors is highly regarded by science and technology. The distinct physical and chemical features of the SiC nanostructures make

them an exciting and attractive class of novel materials with an enormous potential for various applications.[1–6]

SiC nanocrystals have been studied extensively in the last 10 years as a very interesting object for potential application as nanoscale light emitters for blue and UV spectral ranges.[7–9] In addition to the shape and size controlling of the materials in the nanoscale range, the incorporation of atomic impurities is a common way to modify the physical properties of nanostructures. So far some theoretical calculations have been done on the structural, electronic and optical properties of the pure SiC nanocrystals.[10,11] This work presents the calculation results of the nitrogen doped typical SiC nanocrystal for investigating the role of the impurity states on the energy gap and optical properties of this family of materials. This work is organized as follows: in Sec. 2 the theoretical framework we use is briefly described, while Secs. 3 and 4 are respectively devoted to the discussion of the result concerning the electronic and optical properties and our conclusions.



## 2. Computational Details

We study spherical SiC nanocrystals with a diameter of 1.2 nm ($Si_{43}C_{44}H_{76}$) using LCAO in combination with pesudopotential density functional calculation. The SiC nanocrystals have been modeled taking all the cubic bulk SiC atoms contained within a sphere of a given radius and terminating the surface dangling bonds with hydrogen atoms. The structural properties have been determined by allowing all the atoms of each SiC nanocrystal to fully relax. It is worth pointing out that the starting SiC nanocrystals have $T_d$ symmetry. The SiC nanoparticles have been embedded in large supercells in order to prevent interactions between the periodic replicas (about 30 Å of vacuum separate) neighboring nanoparticles in all the considered systems. A careful convergence analysis has been performed on both the electronic and structural properties with respect to the LCAO basis set cutoff. Full geometry optimization was performed with *ab initio* calculations based on the generalized gradient approximation (GGA) with the Perdew–Burke–Erenzerhof (PBE) functional[12] in the density functional theory (DFT) and standard norm-conserving Troullier-Matins Pseudo-potentials.[13] The total energy of the molecular system and Helman–Feynman forces acting on atoms were calculated with convergence tolerance set to $10^{-4}$ eV and 0.05 eV/Å, respectively.

### 2.1. *Theoretical description of method*

In this work we extend the optical response calculations to take into account the effect of the nitrogen as an impurity. We employed the results of our calculations with the optimal basis set to compute the dielectric function of SiC nanocrystals. It is well known that the electric field of the incoming light can polarize the materials using the following relation[14]:

$$P^i(\omega) = \chi^{(1)}_{ij}(-\omega, \omega) \cdot E^j(\omega)\,, \tag{1}$$

where $\chi_{ij}^{(1)}$ is the linear optical susceptibility tensor and it is given by[15]:

$$\chi_{ij}^{(1)}(-\omega,\omega) = \frac{e^2}{\hbar\Omega}\sum_{nm\mathbf{k}} f_{nm}(\mathbf{k})\frac{r_{nm}^i(\mathbf{k})r_{mn}^i(\mathbf{k})}{\omega_{mn}(\mathbf{k})-\omega} = \frac{\varepsilon_{ij}(\omega)-\delta_{ij}}{4\pi}\,. \tag{2}$$

In above relation, the $n$ and $m$ indicate energy bands, $f_{mn}(\mathbf{k}) \equiv f_m(\mathbf{k}) - f_n(\mathbf{k})$ is the Fermi occupation factor, $\Omega$ is the normalized volume. $\omega_{mn}(\mathbf{k}) \equiv \omega_m(\mathbf{k}) - \omega(\mathbf{k})$ is the frequency differences. The $\mathbf{r}_{mn}$ is the matrix elements of the position operator and is given by:

$$r_{nm}^i(\mathbf{k}) = \begin{cases} \dfrac{\nu_{nm}^i(k)}{i\omega_{nm}} & \omega_n \neq \omega_m \\ 0 & \omega_n = \omega_m \end{cases}, \tag{3}$$

where $\nu_{nm}^i(\mathbf{k}) = m^{-1}p_{nm}^i(\mathbf{k})$, $m$ is the free electron mass and $\mathbf{p}_{nm}$ is the momentum matrix element. According to the above relations the dielectric function is defined as:

$$\varepsilon_{ij}(\omega) = 1 + 4\pi\chi_{ij}^{(1)}(-\omega,\omega)\,. \tag{4}$$

The imaginary part ($\varepsilon_2$) of the dielectric function can be obtained by:

$$\varepsilon_2^{ij}(\omega) = \frac{e^2}{\hbar\pi}\sum_{nm}\int d\mathbf{k} f_{nm}(\mathbf{k})\frac{\nu_{nm}^i(\mathbf{k})\nu_{nm}^j(\mathbf{k})}{\omega_{mn}^2}\delta(\omega-\omega_{mn}(\mathbf{k}))\,. \tag{5}$$

Using the Kramers–Kroning transformation the real part of the dielectric function can be expressed by:

$$\varepsilon_1^{ij}(\omega) = \frac{2}{\pi}P\int_0^\infty \frac{\omega'\varepsilon_2^{ij}(\omega')}{\omega'^2-\omega^2}d\omega'\,. \tag{6}$$

The optical response of the hydrogen-terminated SiC nanocrystals was implemented in SIESTA.[16] The optical matrix element was calculated including the corrections due to the nonlocality of the pesudopotential.[17] The refractive index, $n$ and the optical absorption coefficient then can be calculated by the following formula[18]:

$$n = \sqrt{\frac{\sqrt{\varepsilon_1^2(\omega)+\varepsilon_2^2(\omega)}+\varepsilon_1(\omega)}{2}}\,, \tag{7}$$

$$\alpha = 2\frac{\omega}{c}\sqrt{\frac{\sqrt{\varepsilon_1^2(\omega)+\varepsilon_2^2(\omega)}-\varepsilon_1(\omega)}{2}}\,. \tag{8}$$

## 3. Results and Discussion

Due to the fact that the surface effects strongly increase with decreasing size of the material, doping process of the nanostructures may be affected significantly by surface effects. One of the important aspects of the interaction of impurities with a nanostructure is the determination of the most stable positions of the impurity

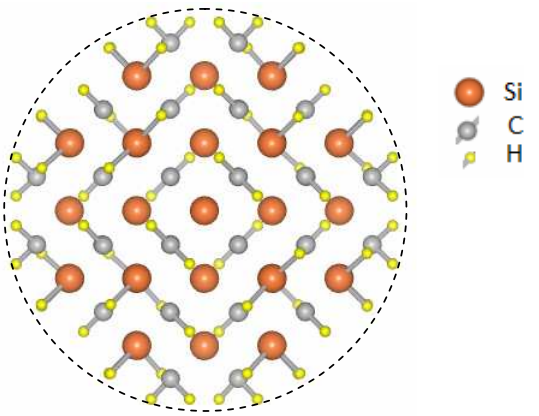


Fig. 1. The optimized geometry of the $Si_{43}C_{44}H_{76}$ nanocrystal.



within atomic structure of the nanomaterials. For small semiconducting nanostructure, such as SiC nanocrystals with a few nanometers doping an impurity can strongly change the optical properties. In our case the nitrogen atom as an impurity atom can penetrate to the internal layers of the SiC nanocrystal, with regard to the minimization of the surface binding energy and atomic force induced to the nanocrystal lattice.

For investigating the electronic and optical properties of the nitrogen doped SiC nanocrystals, a general form of the SiC nanocrystals, i.e., $Si_{43}C_{44}H_{76}$ structure have been selected with $T_d$ symmetry as shown in Fig. 1. The surface dangling bonds have been terminated by the hydrogen atoms. The average C—H, Si—H and Si—C bond lengths after geometry optimization in $Si_{43}C_{44}H_{76}$ are 1.104, 1.508 and 1.879 Å.

For exploring the effect of the nitrogen atom as an impurity in the physical properties of $Si_{43}C_{44}H_{76}$ nanocrystal, we have examined nine possible situations as the nitrogen atom has high probability for replacement in the lattice or it can be placed between atoms in the nanocrystal. The selected nanocrystal has three semi-spherical layers where the same type atoms in each layer have approximately the equivalent position and same distance from the nanocrystal center. We have calculated the binding energy of the nitrogen atom in the optimized geometry of the SiC nanocrystal.

In Fig. 2, the schematic representation of the nitrogen atom locations in the $Si_{43}C_{44}H_{76}$ nanocrystal and the optimized geometry of all the examined structures containing nitrogen as an impurity have been shown. We have labeled the nanocrystal structures with capital letters "A" to "I". The "A" nanocrystal is the pure $Si_{43}C_{44}H_{76}$, while in B, C and D simulated nanocrystals, a carbon atom is substituted by a nitrogen atom. The distance of the nitrogen atom is closed to the nanocrystal center from "B" to "C". In "E", "F" and "G" structures a silicone atom from $Si_{43}C_{44}H_{76}$ nanocrystal is substituted by a nitrogen atom as the distance of

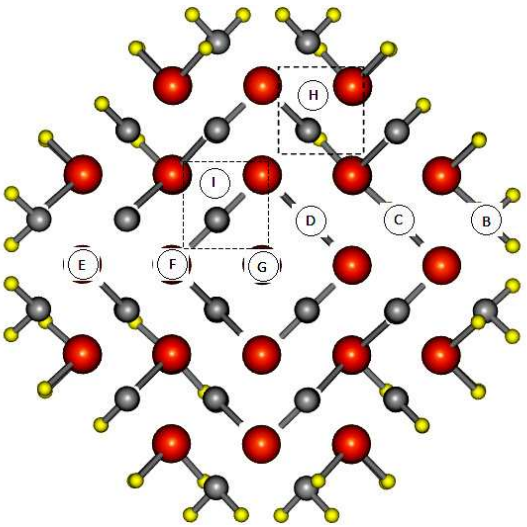


(a)

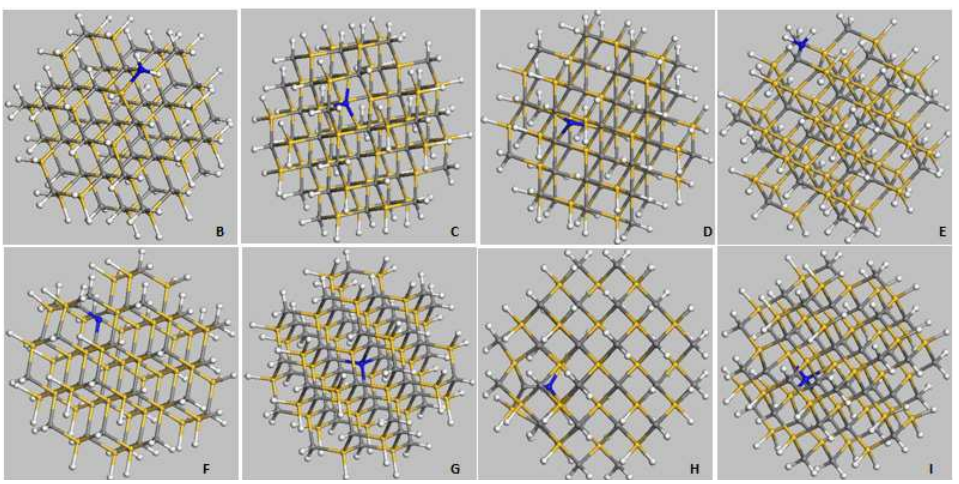


Fig. 2. (a) Schematic representation of the nitrogen atom location in the $Si_{43}C_{44}H_{76}$ nanocrystal, (b) optimized geometry of all the examined structures containing nitrogen impurity.

the nitrogen is close to the nanocrystal center. In the "H" and "I" systems, the complexes of the nanocrystal and nitrogen atom were fully optimized in the conditions that nitrogen atom is placed between first–second and second–third layers. The binding energy can be defined as the difference between the total energy of the doped SiC nanocrystal and the sum of all isolated atom energies which have existed in the system. The negative sign of the binding energy means that the complexes are energetically favorable and one can expect that these complexes really form in experimental conditions.

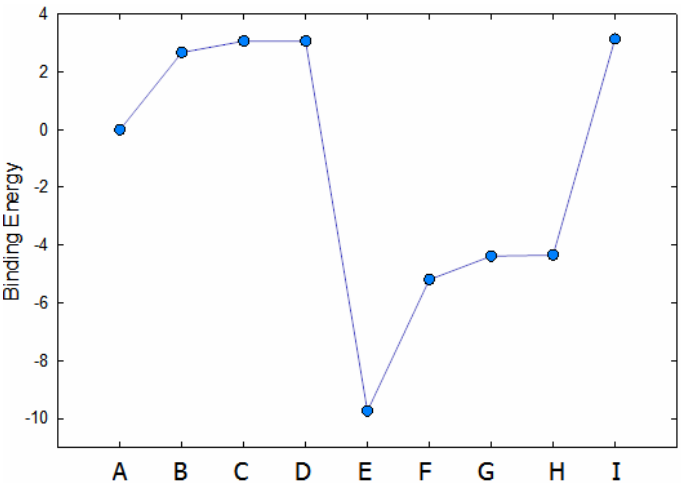


Fig. 3. The nitrogen binding energy in various ($Si_{43}C_{44}H_{76}$, N) systems.

In Fig. 3 the binding energies of the nitrogen atom in all examined structures have been shown. It can be seen that the "E" to "H" structures are energetically favorable and nitrogen atom can bind to the structure in the stable state. Also it is clear from the figure that the "E" system has more stability when a silicon atom is replaced by nitrogen atom in the nanocrystal lattice. The binding energy of nitrogen doped system at "E" state ($Si_{42}NC_{44}H_{76}$) is $-9.74$ eV which is significantly more than the binding energy of nitrogen doped system at "F" ($-5.19$ eV) and "G" ($-4.34$ eV) states. In the case of the "H" state, the nitrogen is placed in the lattice at 3.25 Å from the nanocrystal center. In this case the binding energy of the nitrogen doped system is about $-4.34$ eV which is approximately equal to the "G" system binding energy. As it is clear from Fig. 3 the binding energy of the nitrogen doped "I" system increase rapidly towards positive region, which means that the nitrogen impurity lay between topmost layers of the nanocrystal and for penetrating to the internal layer encounter to the energy barrier about 3.06 eV.

Single impurities can deform strongly the electronic configuration of the systems containing few atoms. The most important role of the impurities in semiconducting systems is the appearance of the new electronic states in the band gap region of the semiconductor. In Fig. 4, the electronic density of states of the $Si_{42}NC_{44}H_{76}$ nanocrystal and its thermodynamically stable doped nitrogen nanocrystals are shown. Also for more considerations, the distribution of the highest occupied molecular orbital (HOMO), lowest unoccupied molecular orbital (LUMO) and impurity states are shown separately for each system as an inset of the Fig. 4. As it can be seen from the Fig. 4(a), the pure SiC nanocrystal ($Si_{43}C_{44}H_{76}$) has a wide band gap of about 6.15 eV. The HOMO and LUMO wavefunction are mainly localized on the carbon "p" orbitals of the nanocrystal within a nearly symmetrical distribution. The calculated density of states for all nitrogen doped stable nanocrystals

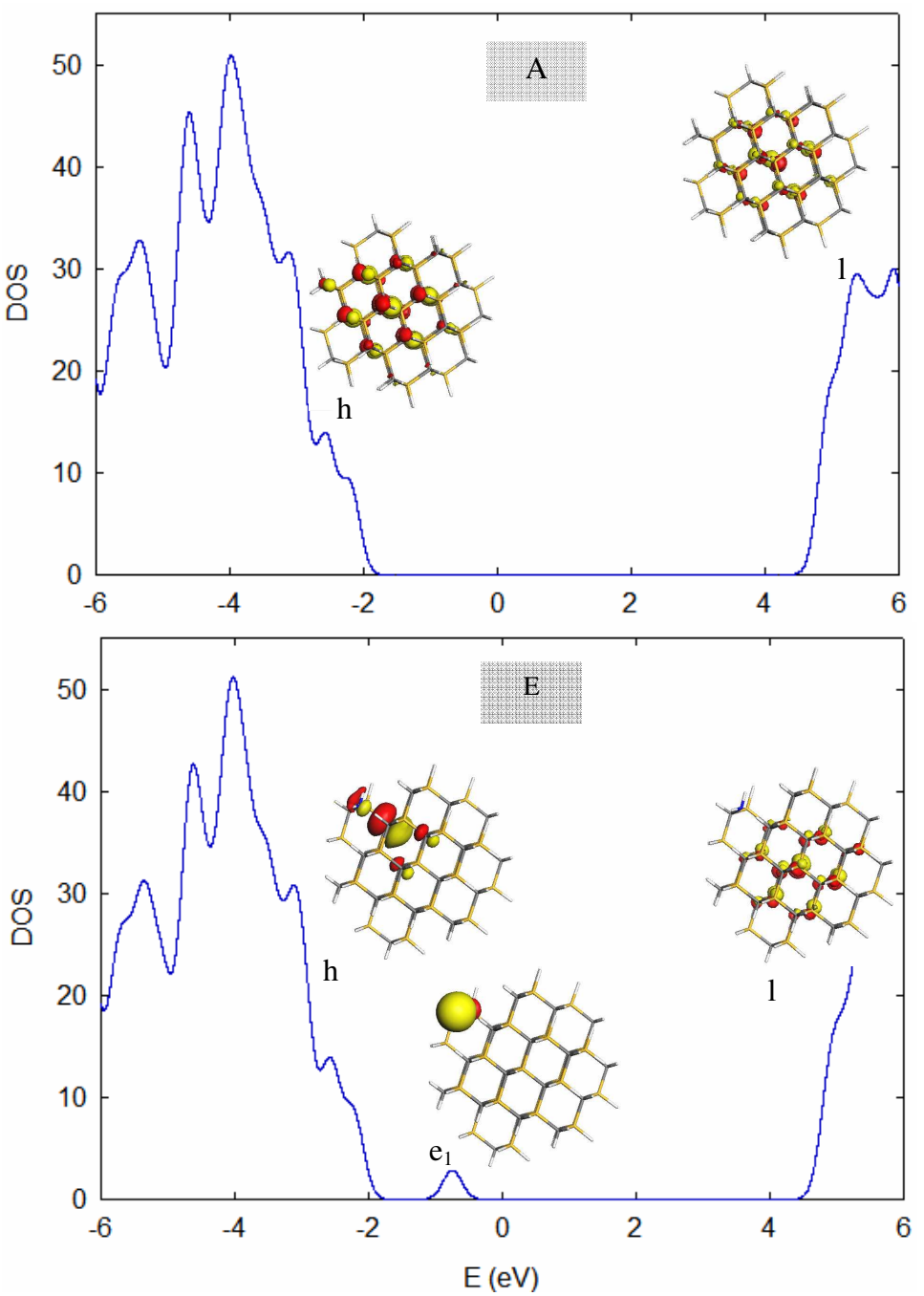


Fig. 4. The calculated density of states of $Si_{43}C_{44}H_{76}$ nanocrystal and its various nitrogen doped configurations. The HOMO, LUMO and impurity state wavefunction are also depicted in the figure.

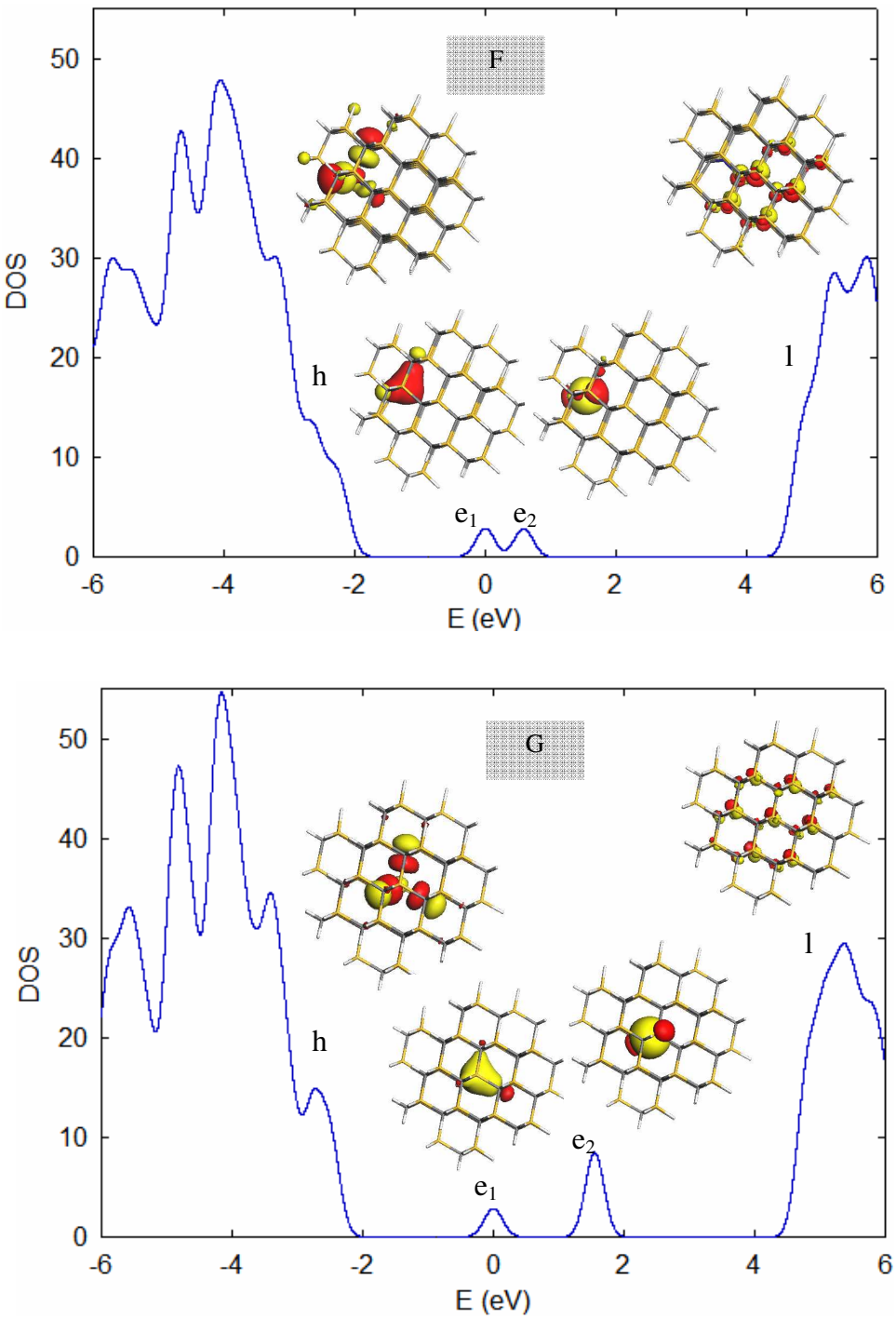


Fig. 4. (*Continued*).

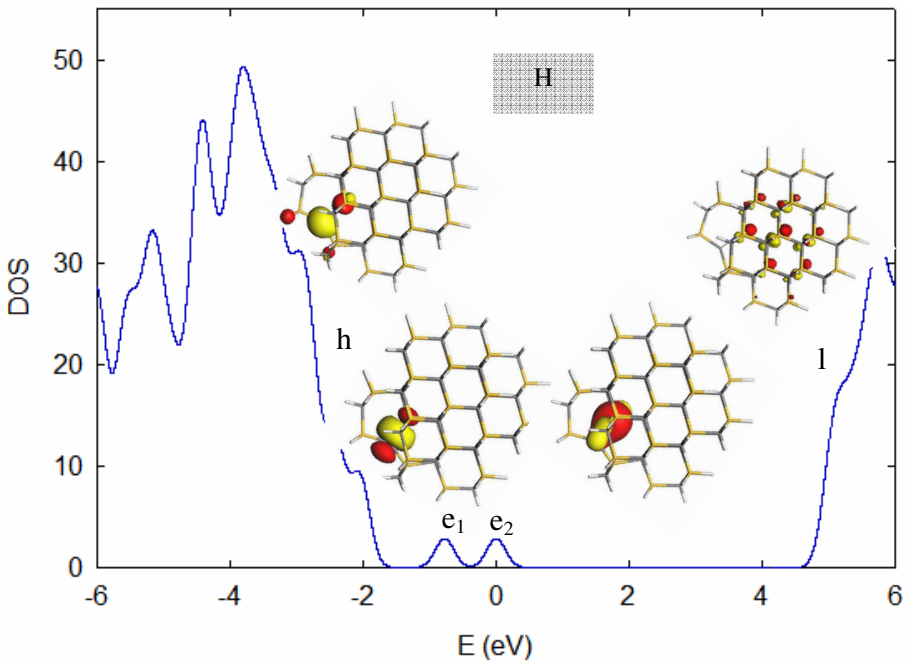


Fig. 4. (*Continued*).



has been shown in Fig. 4(b)–4(e). It is clear from the figure that the new states can form in the gap region of the nitrogen doped nanocrystals. As it is clear from frontier molecular orbital wavefunction projected on each impurity state, all impurity states are extremely localized on the "p" atomic orbitals of the nitrogen atom. A significant event that can be seen from Fig. 4 is that the HOMO levels of the doped nanocrystals are partly under influence of the impurity state while the LUMO levels have not changed significantly. In the case of the "E" system, the nitrogen impurity levels appear at 1.96 eV above the valence band and the HOMO wavefunction is significantly concentrated on the Si and C atoms, close to the nitrogen atom. For "F" and "G" system, the nitrogen atom distance from the nanocrystal center is reduced and the interaction of the nitrogen atomic orbitals with orbitals of the greater number of neighboring atoms increases. So the degeneracy of the "p"-nitrogen orbitals are removed and two separate peaks appear. We have shown the DOS peaks of the impurity states with the symbols of $e_1$ and $e_2$ in which the position of each peak relative to the upper edge of the valence band are listed in Table 1. Another issue that can well be seen in the DOS curve is the shift of the impurity level towards the lower edge of the conduction band when the nitrogen atom position is close to the nanocrystal center. The same behavior can be found in the "H" configuration of doped $Si_{42}NC_{44}H_{76}$ nanocrystal.

With regards to the significant changes in the band gap region of the $Si_{42}NC_{44}H_{76}$ nanocrystal, the study of the optical properties can be useful. The

Table 1. The energy gap (eV) between HOMO ($h$), LUMO ($l$) and impurity energy levels in nitrogen doped various configurations of SiC nanocrystals.

| System | |
|---|---|
| A | $h-l$ (6.68) |
| E | $h-e_1$ (1.52) $e_1-l$ (5.16) $h-l$ (6.68) |
| F | $h-e_1$ (1.97) $h-e_2$ (2.55) $e_1-e_2$ (0.58) $e_1-l$ (4.71) $e_2-l$ (4.13) $h-l$ (6.68) |
| G | $h-e_1$ (1.97) $h-e_2$ (3.49) $e_1-e_2$ (1.52) $e_1-l$ (4.71) $e_2-l$ (3.19) $h-l$ (6.68) |
| H | $h-e_1$ (1.21) $h-e_2$ (2.00) $e_1-e_2$ (0.79) $e_1-l$ (5.47) $e_2-l$ (4.68) $h-l$ (6.68) |



optical absorption and refractive index energy dispersions of the pure and various stable $N$-doped SiC nanocrystals are shown in Figs. 5 and 6. Strong correlation between optical absorption, refractive index and energy gap properties of the nanocrystals can be found. Generally, in all absorption curves, a sizable peak exists in the range of $6-8$ eV. As seen in pure $Si_{43}C_{44}H_{76}$, this peak corresponds to the delocalized HOMO $\rightarrow$ LUMO state vertical excitation. With reference to this fact that the existence of the nitrogen impurity can form new electronic states in the gap, the emergence of significant changes in the absorption spectrum is expected. It can be seen from figure that the new absorption peaks arise due to the electronic excitation from nitrogen impurity states to the conduction band. In Table 2, the location of the main absorption and refractive index peaks and the role of the nitrogen impurity states in vertical excitation were summarized. In the case of the absorption spectrum corresponding to the "E" system, in addition to the main SiC nanocrystal peak two new absorption peaks appear in the spectrum. The origin of these peaks is the vertical excitations of the electronic states from HOMO $\rightarrow e_1(a_1)$ and $e_1 \rightarrow$ LUMO$(a_2)$. In the case of the "F" system, in addition of the main SiC nanocrystal peak two new peaks are added to the absorption spectrum. The first low energy peak corresponds to the electronic transitions of the HOMO $\rightarrow e_1$ and $e_2$ nitrogen impurity states which have been broadened at a region with a size of 0.5 eV. The second peak, which appears at an interval of 4–5.3 eV, is related to the $e_1$ and $e_2 \rightarrow$ LUMO state transition. Finally the last peak refers to the HOMO $\rightarrow$ LUMO transition in the doped SiC nanocrystal. In the case of "G" system, the same behavior can be found. Another remarkable result of the absorption peak analysis can be seen in the "H" system, where the nitrogen atom is placed in the free space between silicone and carbon atoms. It can be seen from Fig. 5 that there are five main absorption peaks, where the first lower peak is related to the interband electronic transition of impurity states namely $e_1 \rightarrow e_2$, the second and third lowest peak is correlated to the HOMO state transition to the two separated nitrogen impurity levels. The forth peak correspond to impurity states transition to the LUMO state and the last peak in the "H" system, as it is seen in all the before considered systems, is the HOMO $\rightarrow$ LUMO transitions. For more considerations, the refractive index of the various nitrogen doped stable SiC nanocrystals was shown in Fig. 6. As it is clear from the figure that there are strong correlation

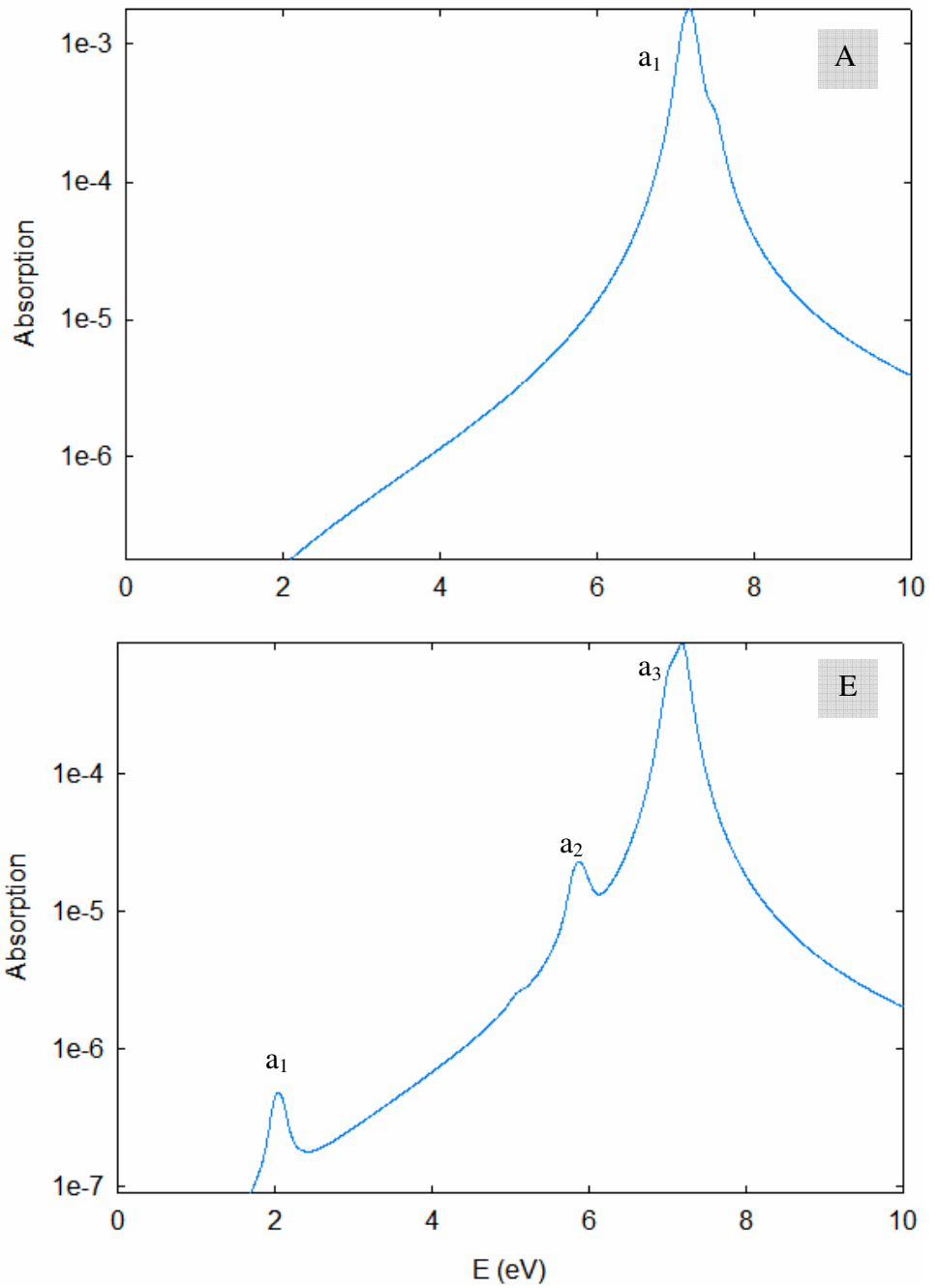


Fig. 5. The calculated absorption coefficient of $Si_{43}C_{44}H_{76}$ nanocrystal in its various nitrogen doped configurations.

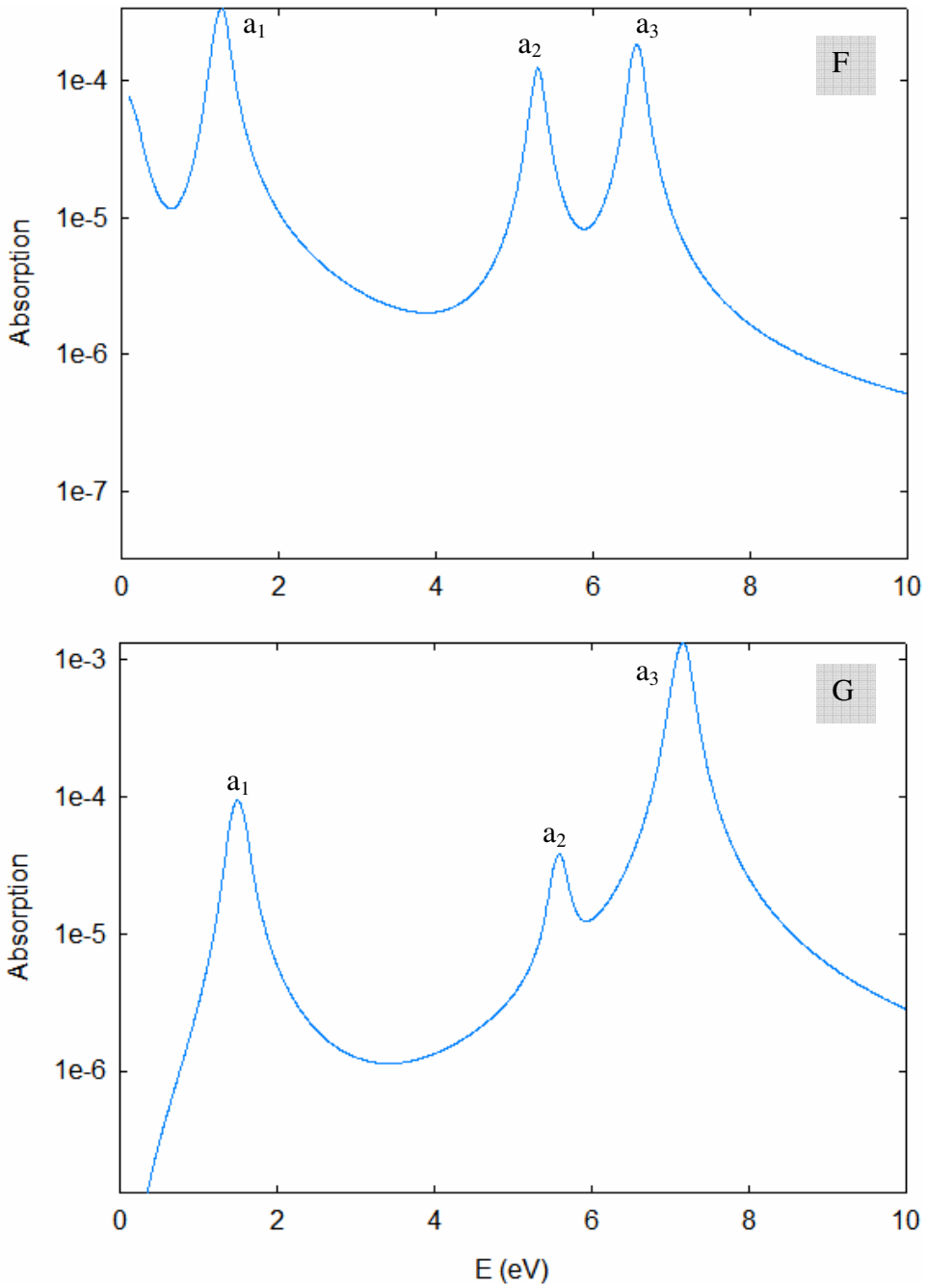


Fig. 5. (*Continued*).

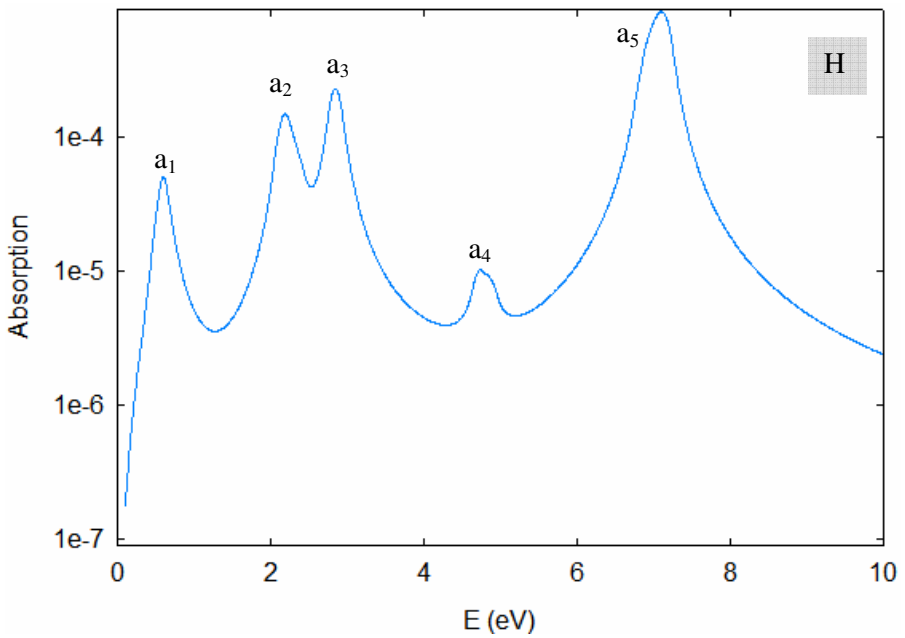


Fig. 5. (*Continued*).

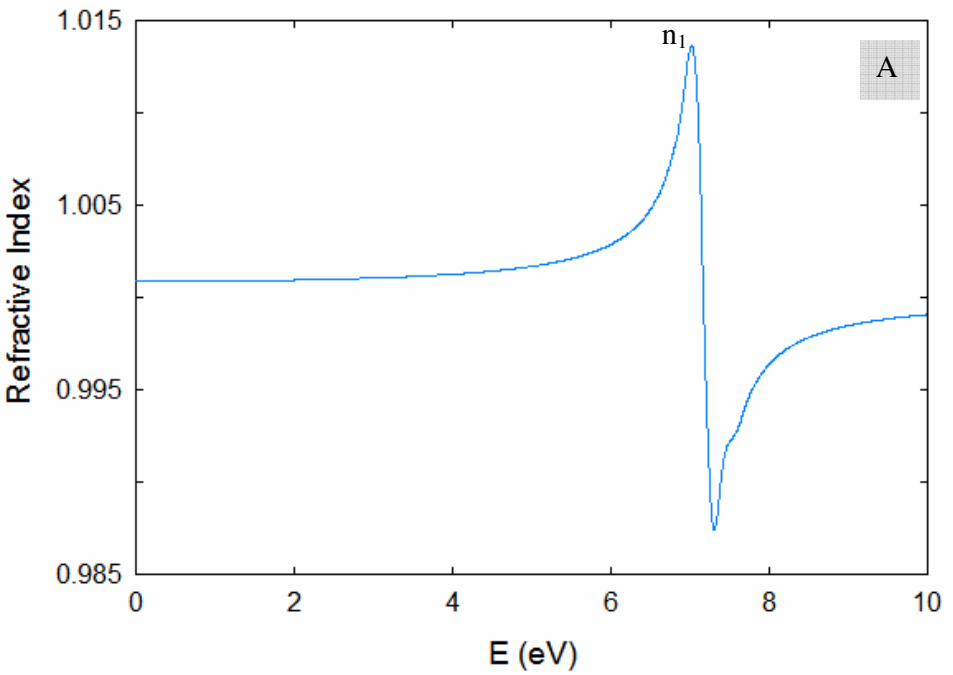


Fig. 6. The calculated refractive index of $Si_{43}C_{44}H_{76}$ nanocrystal and its various nitrogen doped configurations.

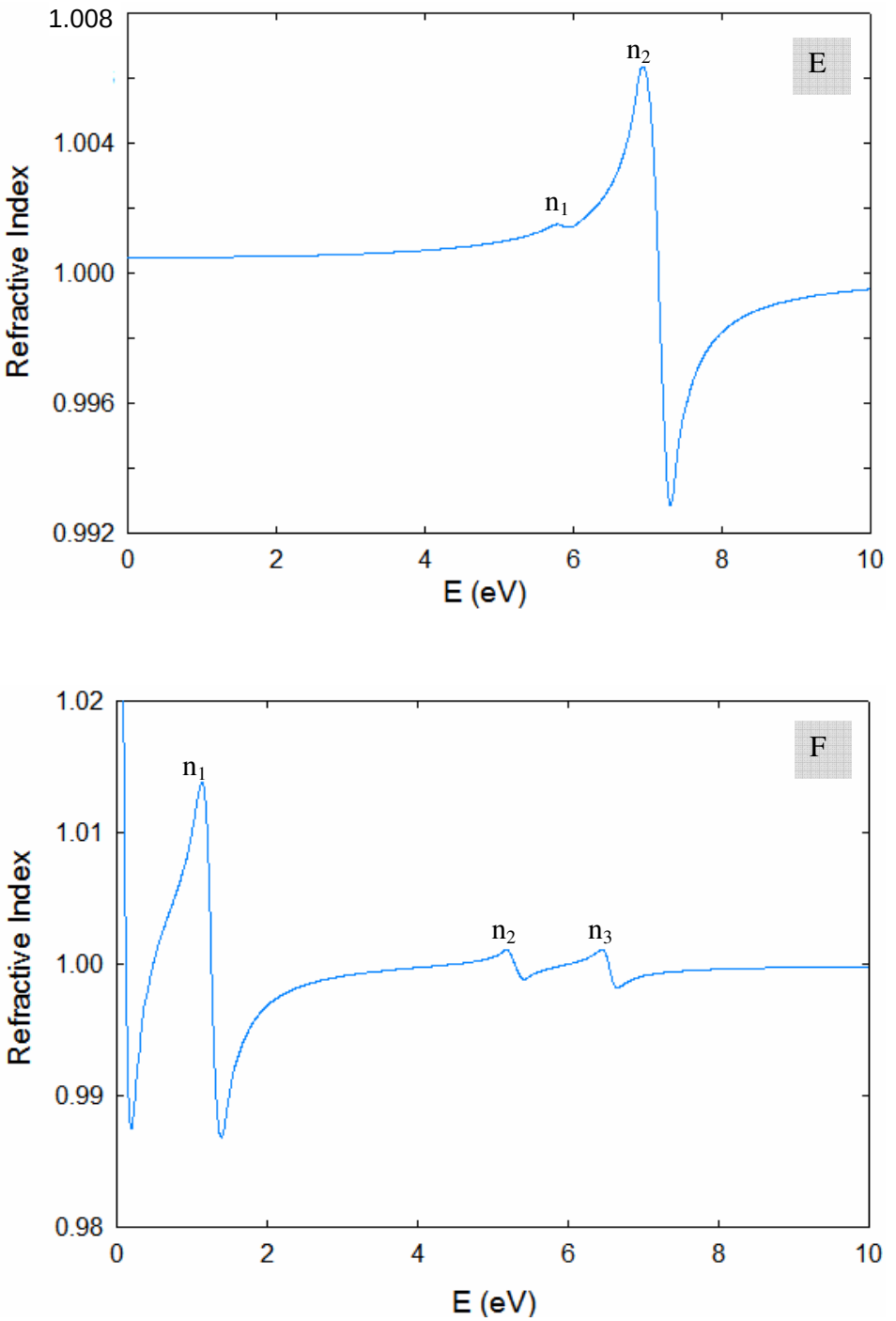


Fig. 6. (*Continued*).

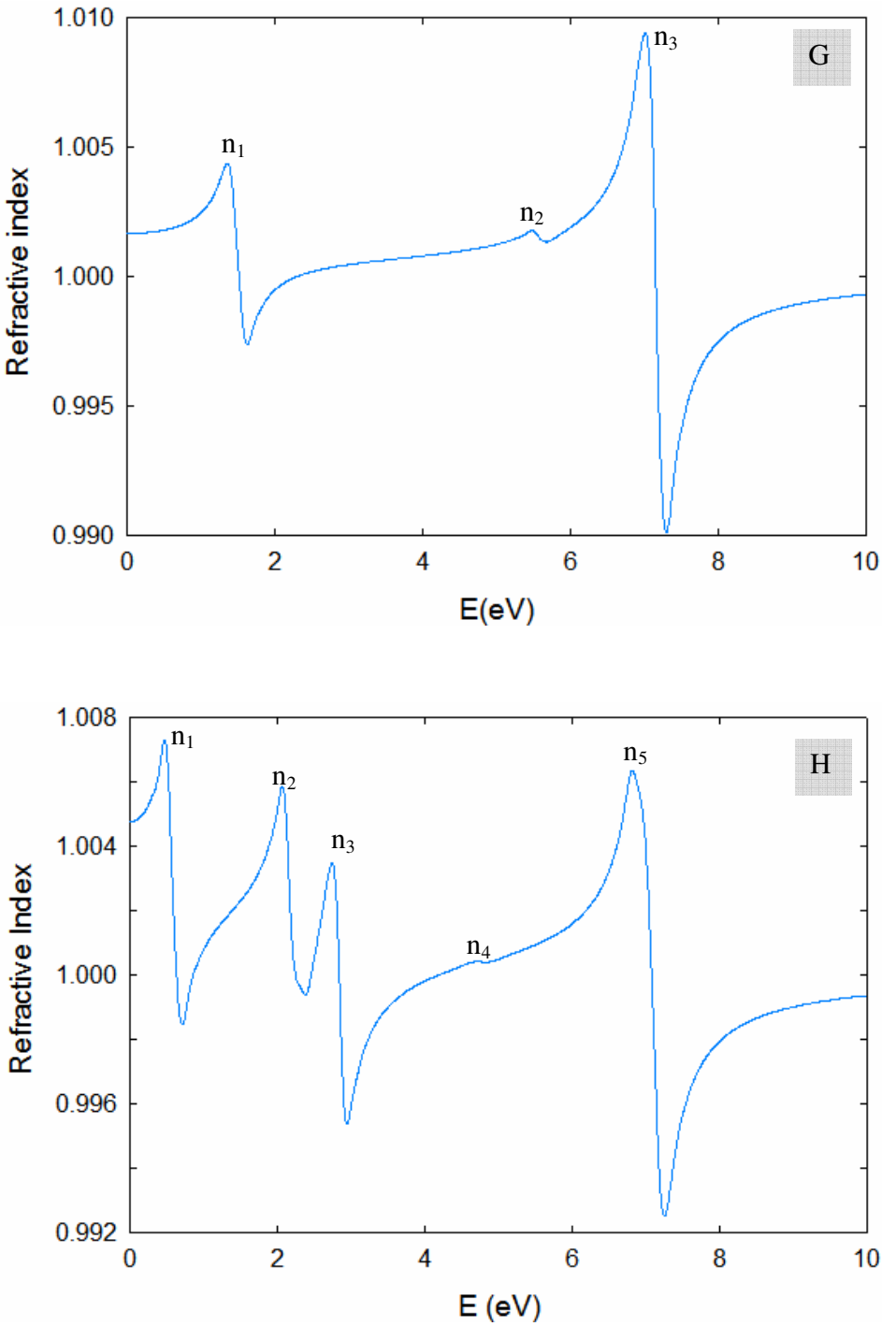


Fig. 6. (*Continued*).

Table 2. The main optical transitions between HOMO ($h$), LUMO ($l$) and impurity energy levels ($e_1$ and $e_2$) in nitrogen doped various configurations of SiC nanocrystals.

| System | | | | | |
|---|---|---|---|---|---|
| A | $n_1, a_1\ (h \to l)$ | | | | |
| E | $n_1, a_1\ (h \to e_1)$ | $n_2, a_2\ (e_1 \to l)$ | $n_3, a_3\ (h \to l)$ | | |
| F | $n_1, a_1\ \{(h \to e_1) + (h \to e_2)\}$ | $n_2, a_2\ \{(e_1 \to l) + (e_2 \to l)\}$ | $n_3, a_3\ (h \to l)$ | | |
| G | $n_1, a_1\ \{(h \to e_1) + (h \to e_2)\}$ | $n_2, a_2\ \{(e_1 \to l) + (e_2 \to l)\}$ | $n_3, a_3\ (h \to l)$ | | |
| H | $n_1, a_1\ (e_1 \to e_2)$ | $n_2, a_2\ (h \to e_1)$ | $n_3, a_3\ (h \to e_2)$ | $n_4, a_4\ \{(e_1 \to l) + (e_2 \to l)\}$ | $n_5, a_5\ (h \to l)$ |

between refractive index dispersion peaks and absorption spectrum. It can be seen that in the case of the "F", "G" and "H" systems the refractive index significantly dispersed from unit value in the range of 0–8 eV.



## 4. Conclusion

We study nitrogen doped spherical SiC nanocrystal with a diameter of 1.2 nm ($Si_{43}C_{44}H_{76}$) using LCAO in combination with pesudopotential density functional calculation. Our selected SiC nanocrystal has been modeled taking all the bulk SiC atoms contained within a sphere of a given radius and terminating the surface dangling bonds with hydrogen atoms. We have examined nine possible situations in which nitrogen has high probability for replacement in the lattice or lies between atoms in the nanocrystal. The selected nanocrystal has three semi-spherical layers where the same type atoms in each layer have approximately equivalent position and same distance from the nanocrystal center. We have found that the silicone can substitute with the nitrogen atom due to minimization of the binding energy in each layer as the constructed nanocrystals remain thermodynamically stable while the carbon sites are not energetically favorable for nitrogen impurity atom. Also the nitrogen atom can place between free atomic spaces as the more thermodynamically stable position of the nitrogen is between the topmost layers. The nitrogen impurity makes changing the electronic structure of the nanocrystal and new electronic state appear in the gap region of the SiC nanocrystal. The position of the impurity energy levels in the gap region changes significantly with the position of the nitrogen in the nanocrystal lattice structure. All new states are extremely localized on the "p" atomic orbitals of the nitrogen atom. The optical absorption and refractive index energy dispersions of the pure and various stable doped SiC nanocrystals were studied. Generally, in all absorption curves, a sizable peak exists at the range of 6–8 eV which is related to the pure $Si_{43}C_{44}H_{76}$ and corresponds to the HOMO $\to$ LUMO state vertical excitation. According to the existence of the new impurity states in the gap region of the nanocrystal, the optical absorption also changes with appearance of the new peaks in the lower energy region. The similar behavior can also be found in refractive index variation regarding the nitrogen doping.

## References

1. J. Botsoa *et al.*, *Appl. Phys. Lett.* **92**, 173902 (2008).
2. J. Fan *et al.*, *Small* **4**, 1058 (2008).

3. F. Reboredo, L. Pizzagalli and G. Galli, *Nano Lett.* **4**, 801 (2004).
4. Z. Makkai *et al.*, *Appl. Phys. Lett.* **86**, 253109 (2005).
5. X. H. Peng *et al.*, *J. Appl. Phys.* **102**, 024304 (2007).
6. X. L. Wu *et al.*, *Phys. Rev. Lett.* **94**, 026102 (2005).
7. T. Matsumoto *et al.*, *Appl. Phys. Lett.* **64**, 226 (1994).
8. L. S. Liao *et al.*, *Appl. Phys. Lett.* **66**, 2382 (1995).
9. T. V. Torchynska *et al.*, *Microelectronics* **36**, 536 (2005).
10. S. L. Shi *et al.*, *Thin Solid Films* **495**, 404 (2006).
11. M. Voros *et al.*, *Appl. Phys. Lett.* **96**, 051909 (2010).
12. J. P. Perdew, S. Burke and M. Ernzerhof, *Phys. Rev. Lett.* **77**, 3865 (1999).
13. N. Troullier and J. L. Martins, *Phys. Rev. B* **43**, 1993 (1991).
14. Z. H. Levine and D. C. Allan, *Phys. Rev. Lett.* **63**, 1719 (1989).
15. H. Philipp and R. H. Ehrenreich, *Phys. Rev.* **129**, 1550 (1963).
16. J. M. Soler *et al.*, *J. Phys.: Condens. Matter* **14**, 2745 (2002).
17. A. J. Read and R. J. Needs, *Phys. Rev. B* **44**, 13071 (1991).
18. D. J. Griffiths, *Introduction to Electrodynamics* (Prentice Hall, New Jersey, 1999).